Electronic Supplementary Material (ESI) for Physical Chemistry Chemical Physics.

Isolating the role of hydrogen bonding in hydroxyl-functionalized ionic liquids by means of vaporization enthalpies, infrared spectroscopy and molecular dynamics simulations

Dzmitry H. Zaitsau,[a,b] Jan Neumann, Thomas Niemann,[a] Anne Strate,[a,b] Dietmar Paschek,[a,b*] Sergey P. Verevkin,[a,b*] and Ralf Ludwig,[a,b,c*]

[a] Universität Rostock, Institut für Chemie, Abteilung für Physikalische Chemie, Dr.-Lorenz-Weg 2, 18059, Rostock, Germany

[b] Department LL&M, University of Rostock, Albert-Einstein-Str. 25, 18059, Rostock, Germany

[c] Leibniz-Institut für Katalyse an der Universität Rostock e.V., Albert-Einstein-Str. 29a, 18059 Rostock, Germany

Contents

1. Materials and Synthesis

Sample preparation

Synthesis of the onium salts: Equimolar amounts of the heterocyclic amine and 2-bromoethanol, 3-chloropropanol or 1-bromopropane respectively were mixed and heated up to 110 °C for 1h. Upon cooling, the mixture began to crystallize. The crude product was recrystallized from acetone/acetonitrile mixtures to obtain the colorless crystalline product.
Synthesis of the bis(trifluoromethanesulfonyl)imide: Equimolar amounts of the onium halide and lithium-bis(trifluoromethanesulfonyl)imide were mixed as aqueous solutions for 1h. Two phases were obtained, the lower one was washed several times with water until no residual bromine could be detected with silver nitrate solution. The obtained colorless liquids were dried for several hours in vacuum at 60 °C.
All 3-methylimidazolium based ILs were purchased from IoLiTec and dried for several hours in vacuum at 60 °C.

Synthesis of the specific compounds

Apart from the reactions in aqueous solutions all reactions were performed in a moisture-guarded assembly and reflux condenser was used while heating. The used solvents were dried with molecular sieves to a water content less than 50 ppm and distilled freshly. All starting materials used in the synthesis were purchased from Sigma Aldrich and dried by conventional methods for the use in moisture-free reactions.

1-(2-Hydroxyethyl)pyridinium-bromide [HEPy][Br]

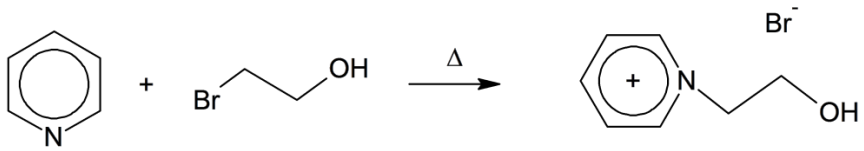

At room temperature equimolar amounts of pyridine (8.977 g; 113 mmol; 9.6 ml) and 2-bromoethanol (14.929 g; 113 mmol; 14.9 ml) were mixed and heated slowly up to 110 °C. When the reaction begins, the solution turns brown and starts to crystallize. The mixture was cooled to room temperature. The crude product was recrystallized from about 330 ml acetonitrile. The product (**[HEPy][Br]**) was obtained as rod-shaped colorless crystals. Yield 89 %.
EA % cal. (exp.): C 41.20 (41.22); H 4.94 (4.92); N 6.86 (6.76). ^{1}**H-NMR**(298.2 K, DMSO-d6, 300.13 MHz, [ppm]): δ = 3.86 (dd, 2H, CH_2-CH_2-OH); 4.67-4.74 (m, 2H, CH_2-CH_2-OH); 5.25(t, 1H, O*H*); 8.14-8.21 (m, 2H, *m*-C*H*); 8.60-8.67 (m, 1H, *p*-C*H*); 9.03-9.09 (m, 2H, *o*-C*H*). ^{13}**C-NMR**(298 K, DMSO-d6, 75.46 MHz, [ppm]): δ = 59.98 (s, CH_2-CH_2-OH); 63.04 (s, CH_2-CH_2-OH); 127.67 (s, *m*-*C*H); 145.15 (s, *p*-*C*H); 145.53 (s, *o*-*C*H).

1-(2-Hydroxyethyl)pyridinium-bis(trifluoromethanesulfonyl)imide [HEPy][NTf_2]

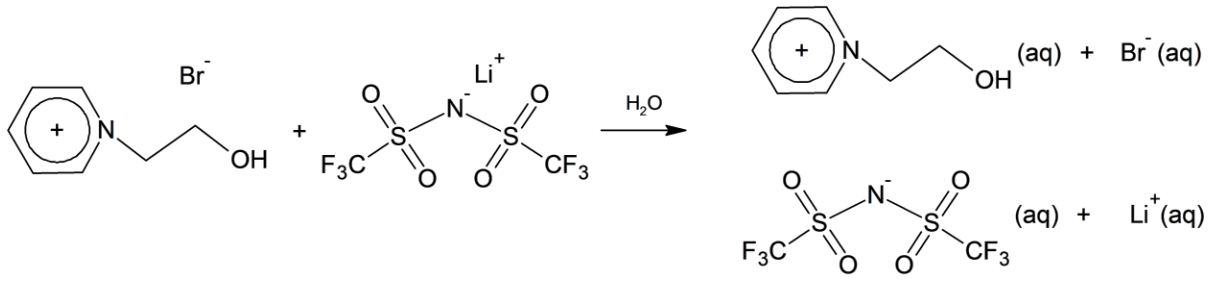

3.220 g (**[HEPy][Br]**) (16 mmol) solved in 2 ml H_2O were added to a solution of 4.576 g lithium- bis(trifluoromethylsulfonyl)imide $LiNTf_2$ (16 mmol) in 2.5 ml H_2O. The mixture was stirred for 1 h. Two phases were obtained, the lower one was washed several times with water until no residual bromine could be detected with silver nitrate solution. The obtained colorless liquid of (**[HEPy][NTf_2]**) was dried for 8 h in vacuum at 60 °C. Yield 57 %.

EA % cal. (exp.): C 26.73 (26.14); H 2.49 (2.41); N 6.93 (6.54); S 15.86 (15.50). ^{1}**HNMR**(298.2 K, DMSO-d_6, 300.13 MHz, [ppm]): δ = 3.88 (dd, 2H, CH_2-CH_2-OH); 4.65- 4.71 (m, 2H, CH_2-CH_2-OH); 5.22(t, 1H, O*H*); 8.12-8.20 (m, 2H, *m*-C*H*); 8.57-8.64 (m, 1H, *p*-C*H*); 9.00-9.05 (m, 2H, *o*-C*H*). ^{13}**C-NMR**(298 K, DMSO-d_6, 75.46 MHz, [ppm]): δ = 59.95 (s, CH_2-CH_2-OH); 63.01 (s, CH_2-CH_2-OH); 119.43 (q, CF_3); 127.65 (s, *m*-CH); 145.12 (s, *p*-CH); 145.50 (s, *o*-CH). ^{19}**F-NMR**(298 K, DMSO-d_6, 282.40 MHz, [ppm]): δ = −78.81 (s, CF_3). **IR** (Transm., CaF_2-Window, 12 μm Spacer, 20 °C, 128 Scans, [cm^{-1}]): 3528 (vw); 3141 (vw); 3097 (vw); 3074 (vw); 2972 (vw); 2951 (vw); 2893 (vw); 2857 (vw); 1936 (vw); 1850 (vw); 1741 (vw); 1638 (w); 1585 (vw); 1502 (vw); 1491 (m); 1451 (vw); 1352 (vs); 1200 (s); 1136 (s); 1060 (s).

1-(3-Hydroxypropyl)pyridinium chloride [HPPy][Cl]

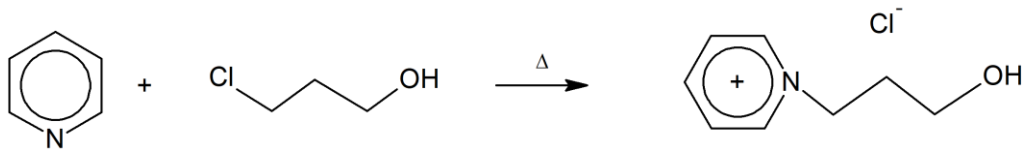

At room temperature equimolar amounts of pyridine (12.231 g; 155 mmol; 13.1 ml) and 3-chloropropanol (14.600 g; 154 mmol; 12.9 ml) were mixed and heated slowly up to 100 °C. When the reaction begins, the solution turns slightly brown and starts to crystallize upon cooling to room temperature . The crude product was recrystallized from about 450 ml acetonitrile. The product was obtained as rod-shaped colorless crystals. Yield 92 %.

^{1}**H-NMR**(298.2 K, DMSO-d_6, 300.13 MHz, [ppm]): δ = 2.03-2.13 (tt, 2H, $CH_2-CH_2-CH_2-OH$); 3.38-3.45 (dt, 2H, $CH_2-CH_2-CH_2-OH$); 4.76 (t, 2H, $CH_2-CH_2-CH_2-OH$); 5.12 (t, 1H, O*H*); 8.13-8.19 (m, 2H, *m*-C*H*); 8.58-8.65 (m, 1H, *p*-C*H*); 9.25-9.29 (m, 2H, *o*-C*H*). ^{13}**C-NMR** (298 K, DMSO-d_6, 75.46 MHz, [ppm]): δ = 33.46 (s, $CH_2-CH_2-CH_2-OH$); 56.88 (s, $CH_2-CH_2-CH_2-OH$); 58.42 (s, $CH_2-CH_2-CH_2-OH$); 127.87 (s, *m*-CH); 145.05 (s, *p*-CH); 145.38 (s, *o*-CH). **IR** (ATR, 30°C, 128 Scans, [cm^{-1}]): 3277 (m); 3128 (w); 3093 (w); 3071 (w); 3043 (w); 3019 (w); 2969 (w); 2939 (w); 2905 (w); 2868 (w); 2804 (w); 1636 (w); 1626 (m); 1579 (vw); 1505 (w); 1484 (s); 1470(m); 1421 (w); 1379 (vw); 1360 (w); 1304 (m); 1265 (w); 1233 (w); 1174 (m); 1150 (w); 1083 (m); 1050 (s); 957 (w); 934(m); 872(vw); 819 (w); 774 (s); 6855 (vs); 638 (s).

1-(3-Hydroxypropyl)pyridinium-bis(trifluoromethanesulfonyl)imide [HPPy][NTf$_2$]

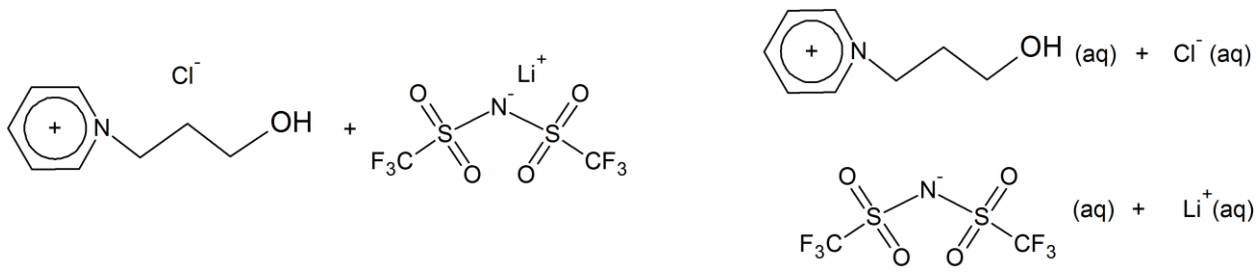

9.653 g (**[HPPy][Cl]**) (56 mmol) solved in 10 ml H_2O were added to a solution of 16.125 g lithium- bis(trifluoromethylsulfonyl)imide $LiNTf_2$ (56 mmol) in 10 ml H_2O. The mixture was stirred for 1 h. Two phases were obtained, the lower one was washed several times with water until no residual chlorine could be detected with silver nitrate solution. The obtained colorless liquid of (**[HPPy][NTf$_2$])** was dried for 8 h in vacuum at 60 °C. Yield 77 %.
^{1}**H-NMR**(298.2 K, DMSO-d$_6$, 300.13 MHz, [ppm]): δ = 2.03-2.13 (tt, 2H, $CH_2-CH_2-CH_2-OH$); 3.41-3.48 (dt, 2H, $CH_2-CH_2-CH_2-OH$); 4.71 (t, 2H, $CH_2-CH_2-CH_2-OH$); 4,88 (t, 1H, O*H*); 8.11-8.19 (m, 2H, *m*-C*H*); 8.56-8.64 (m, 1H, *p*-C*H*); 9.10-9.17 (m, 2H, *o*-C*H*). ^{13}**C-NMR**(298 K, DMSO-d$_6$, 75.46 MHz, [ppm]): δ = 33.27 (s, $CH_2-CH_2-CH_2-OH$); 57.04 (s, $CH_2-CH_2-CH_2-OH$); 58.59 (s, $CH_2-CH_2-CH_2-OH$); 119.43 (q, CF_3); 127.87 (s, *m*-C*H*); 144.99 (s, *p*-C*H*); 145.37 (s, *o*-C*H*). ^{19}**F-NMR**(298 K, DMSO-d$_6$, 282.40 MHz, [ppm]): δ = −78.81 (s, CF_3). **IR** (Transm., CaF_2-Window, 12 μm Spacer, 20 °C, 128 Scans, [cm^{-1}]): 3552 (w); 3299 (m); 3139 (w); 3097 (w); 3071 (w); 2943 (w); 2881 (w); 1637 (m); 1491 (m); 1318 (w); 1286 (w); 1221 (w); 1170 (w); 1060 (vs); 953 (w).

1-Propylpyridinium-bromide [PPy][Br]

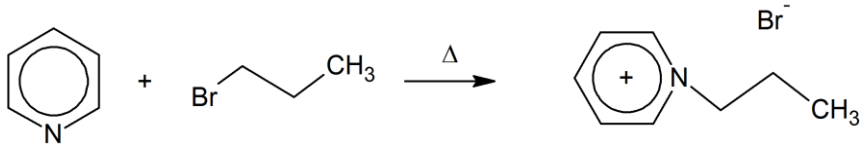

At room temperature equimolar amounts of pyridine (19.57 g; 247 mmol; 20 ml) and 1-bromopropane (30.378 g; 247 mmol; 22.5 ml) were mixed and heated slowly up to 100 °C. When the reaction begins, the solution turns brown and begins to crystallize while cooling to room temperature. The crude product was dispersed in 300 ml ethyl acetate and filtered. The product (**[PPy][Br]**) was obtained as white powder. Yield 91 %.
^{1}**H-NMR**(298.2 K, DMSO-d6, 300.13 MHz, [ppm]): δ = 0.90 (t, 2H, $CH_2-CH_2-CH_3$); 1.86-2.09 (m, 2H, $CH_2-CH_2-CH_3$); 4.61-4.72 (m, 2H, $CH_2-CH_2-CH_3$);
8.19-8.26 (m, 2H, *m*-C*H*); 8.66-8.72 (m, 1H, *p*-C*H*); 9.21-9.30 (m, 2H, *o*-C*H*).
^{13}**C-NMR**(298 K, DMSO-d6, 75.46 MHz, [ppm]): δ = 10.23 (s, $CH_2-CH_2-CH_3$); 23.98 (s, $CH_2-CH_2-CH_3$); 62.04 (s,$CH_2-CH_2-CH_3$); 127.67 (s, *m*-C*H*); 145.19 (s, *p*-C*H*); 145.55 (s, *o*-C*H*).

1-Propylpyridinium-bis(trifluoromethanesulfonyl)imide [PPy][NTf$_2$]

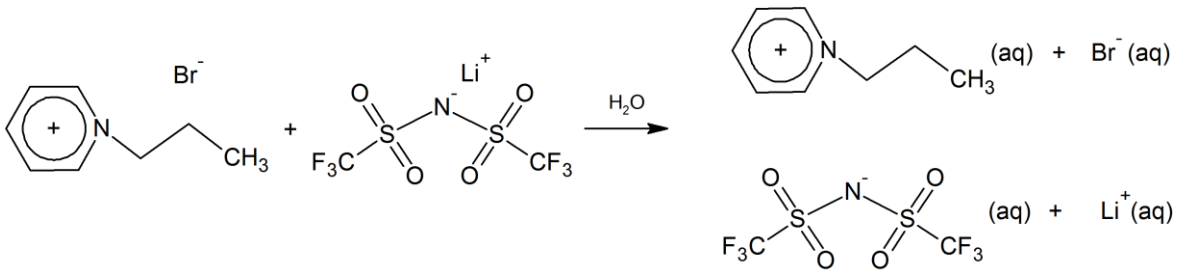

22.10 g (**[PPy][Br]**) (109 mmol) solved in 20 ml H_2O were added to a solution of 31.811g lithium- bis(trifluoromethylsulfonyl)imide $LiNTf_2$ (109 mmol) in 20 ml H_2O. The mixture was stirred for 1 h. Two phases were obtained, the lower one was washed several times with water until no residual bromine could be detected with silver nitrate solution. The obtained colorless liquid of (**[PPy][NTf_2])** was dried for 8 h in vacuum at 60 °C. Yield 83 %.

^{1}**H-NMR**(298.2 K, DMSO-d6, 300.13 MHz, [ppm]): δ = 0.92 (t, 2H, $CH_2-CH_2-CH_3$); 1.87-2.10 (m, 2H, $CH_2-CH_2-CH_3$); 4.61-4.72 (m, 2H, $CH_2-CH_2-CH_3$); 8.19-8.27 (m, 2H, *m*-C*H*); 8.66-8.73 (m, 1H, *p*-C*H*); 9.21-9.31 (m, 2H, *o*-C*H*).

^{13}**C-NMR**(298 K, DMSO-d6, 75.46 MHz, [ppm]): δ = 10.22 (s, $CH_2-CH_2-CH_3$); 24.01 (s, $CH_2-CH_2-CH_3$); 62.10 (s,$CH_2-CH_2-CH_3$); 119.44 (q, CF_3); 127.66 (s, *m*-CH); 145.19 (s, *p*-CH); 145.57 (s, *o*-CH). ^{19}**F-NMR**(298 K, DMSO-d_6, 282.40 MHz, [ppm]): δ = −78.85 (s, CF_3).

2. Vapor pressure and enthalpy of vaporization determiation by usin Quartz-Crystal-Microbalance Langmuir technique.

Vapor pressures and standard molar enthalpies of vaporization of stuied series of ILs were determined by using the QCM method.[1] Vaporization enthalpies were derived from the temperature dependencies of the experimentally measured shift in the vibrational frequency of the quartz crystal. In our method a sample of an IL is placed in an open cavity (Langmuir evaporation) inside of the thermostat block and it is exposed to vacuum (10^{-5} Pa) with the whole open surface of the loaded compound. The QCM is placed directly above the measuring cavity containing the sample. During the vaporization into a vacuum, a certain amount of sample is deposited on the quartz crystal. The change of the vibrational frequency Δf was directly related to the mass deposition Δm on the crystal according to the Sauerbrey equation:[2]

$$\Delta f = - C \cdot f^2 \cdot \Delta m \cdot S_C^{-1} \quad (1)$$

where f is the fundamental frequency of the crystal (6 MHz in this case) with $\Delta f << f$, S_C is the surface of the crystal, and C is a constant.[3] The measured frequency change rates ($df \cdot dt^{-1}$) can be used for calculation of absolute vapor pressures p_{sat} according to the equation:

$$p_{sat} = K' \frac{df}{dt} \sqrt{\frac{T}{M}}. \quad (2)$$

where the $K´ = (9.5 \pm 1.1) \times 10^{-6}$ Pa·s·kg$^{1/2}$·Hz^{-1}·K$^{-1/2}$·mol$^{-1/2}$ is the empirical constant containing all parameters of the Sauerbrey equation as well as the parameters specific for the geometry of the experimental setup.[3] The $K´$-value for our apparatus was evaluated with the help of reliable vapor pressure data available for imidazolium and pyridinium based Ils.[3] Using the experimental vapor pressures p_{sat} measured with the QCM technique the molar enthalpy of vaporization, $\Delta_l^g H_m^o(T)$ at experimental temperatures is obtained according to the Clarke-Glew equation:[4]

$$R\ln(p_{sat}/p^o) = -\frac{\Delta_l^g G_m^\circ(T_{av})}{T_{av}} + \Delta_l^g H_m^\circ(T_{av})\left(\frac{1}{T_{av}} - \frac{1}{T}\right) + \Delta_l^g C_{p,m}^\circ\left(\frac{T_{av}}{T} - 1 + \ln\left(\frac{T}{T_{av}}\right)\right) \quad (3),$$

where T_{av} is the average temperature interval of the study. The value $\Delta_l^g C_{p,m}^o = C_{p,m}^o(g) - C_{p,m}^o(liq)$ is the difference between the molar heat capacities of the gaseous, $C_{p,m}^o(g)$, and the liquid phase, $C_{p,m}^o(liq)$, respectively. The vaporization enthalpy $\Delta_l^g H_m^o(298.15\ K)$ at the reference temperature is calculated according to the Kirchhoff´s equation:

$$\Delta_l^g H_m^o(298.15\ K) = \Delta_l^g H_m^o(T_{av}) + \Delta_l^g C_{p,m}^o\ (298.15 - T_{av}) \quad (4),$$

To detect and avoid any possible effect of impurities on the measured frequency loss rate ($df \cdot dt^{-1}$), a typical experiment was performed in a few consequent series with increasing and decreasing temperature steps. Every series consisted of 5 to 8 temperature points of mass loss rate determination. Several runs have been performed to test the reproducibility of the results. The study

was finished when the enthalpy of vaporization, $\Delta_l^g H_m^o(T_{av})$, obtained in the sequential runs by adjusting Eq. 3 to the temperature dependent rates ($df \cdot dt^{-1}$) agreed within the assessed experimental uncertainty of about ± 1 kJ·mol^{-1}. In order to confirm the absence of decomposition of IL under the experimental conditions, the residual IL in the crucible and the IL-deposit on QCM were analyzed by ATR-FTIR spectroscopy. No changes in the spectra have been detected. Primary experimental results of the QCM studies are given in Table S1. The final uncertainty of the absolute vapor pressure determination is estimated to be 50 % and mostly determined by the uncertainty of *K′* coefficient.

Table S1. The results of the temperature dependence of frequency shift velocity *df/dt* of the QCM for studied Ionic Liquids and, corresponding vaporization enthalpies $\Delta_l^g H^o_m(T)$.[a]

Run	T / K	df/dt / Hz·s^{-1}	$10^6 \cdot p_{sat}$ / Pa	T^{-1} / K^{-1}	$R \cdot \ln(p_{sat}/p^o)$	$\frac{\Delta_l^g H_m^o(T)}{\text{kJ·mol}^{-1}}$
[PMIm][NTf$_2$]						
$\ln(p^*_{sat}/p^o) = -\frac{69296}{RT_0} - \frac{121408}{R}\left(\frac{1}{T} - \frac{1}{T_0}\right) - \frac{76}{R}\left(\frac{T_0}{T} - 1 - \ln\left(\frac{T}{T_0}\right)\right)$, T_0 = 380.2 K, p^o = 10^5 Pa						
1	401.66	0.7738	231	0.002490	-165.3	119.8
	396.77	0.4986	148	0.002520	-169.0	120.2
	391.91	0.3211	95	0.002552	-172.7	120.5
	386.93	0.2010	59	0.002584	-176.7	120.9
	381.95	0.1237	36	0.002618	-180.8	121.3
	376.96	0.07469	22	0.002653	-185.0	121.7
	371.65	0.04272	12	0.002691	-189.7	122.1
	366.36	0.02447	7.0	0.002730	-194.4	122.5
2	394.39	0.3939	117	0.002536	-171.0	120.3
	389.43	0.2529	74.5	0.002568	-174.8	120.7
	384.48	0.1577	46	0.002601	-178.7	121.1
	379.47	0.09743	28	0.002635	-182.8	121.5
	374.49	0.05970	17	0.002670	-186.9	121.8
	369.51	0.03392	10	0.002706	-191.7	122.2
	364.53	0.02072	5.9	0.002743	-195.8	122.6

	359.55	0.01125	3.2	0.002781	-201.0	123.0

[PMIm][OTf]

$\ln(p^*_{sat}/p^o) = -\frac{76900}{RT_0} - \frac{125184}{R}\left(\frac{1}{T} - \frac{1}{T_0}\right) - \frac{70}{R}\left(\frac{T_0}{T} - 1 - \ln\left(\frac{T}{T_0}\right)\right)$, T_0 = 403.7 K, p^o = 10^5 Pa

1	428.09	0.2486	93	0.002336	-172.9	123.5
	423.06	0.1663	62	0.002364	-176.3	123.8
	418.03	0.10827	40	0.002392	-179.9	124.2
	413.00	0.06999	26	0.002421	-183.6	124.5
	407.96	0.04442	16	0.002451	-187.4	124.9
	402.94	0.02848	10	0.002482	-191.1	125.2
	397.91	0.01801	6.5	0.002513	-195.0	125.6
	392.90	0.01105	4.0	0.002545	-199.1	125.9
	387.94	0.006890	2.5	0.002578	-203.1	126.3
	383.04	0.004238	1.5	0.002611	-207.2	126.6
2	425.57	0.2050	77	0.002350	-174.5	123.7
	420.55	0.1339	50	0.002378	-178.1	124.0
	415.52	0.08687	32	0.002407	-181.7	124.4
	410.49	0.05618	21	0.002436	-185.4	124.7
	405.44	0.03565	13	0.002466	-189.3	125.1
	400.43	0.02260	8.2	0.002497	-193.1	125.4
	395.39	0.01390	5.0	0.002529	-197.2	125.8
	390.37	0.008873	3.2	0.002562	-201.0	126.1
	385.38	0.005367	1.9	0.002595	-205.2	126.5
	380.43	0.003196	1.1	0.002629	-209.6	126.8

[PMIm][OMs]

$\ln(p^*_{sat}/p^o) = -\frac{78930}{RT_0} - \frac{135784}{R}\left(\frac{1}{T} - \frac{1}{T_0}\right) - \frac{75}{R}\left(\frac{T_0}{T} - 1 - \ln\left(\frac{T}{T_0}\right)\right)$, T_0 = 399.2 K

1	413.33	0.04559	19	0.002419	-186.2	134.7
	408.36	0.02926	12	0.002449	-190.0	135.1
	403.37	0.01760	7.2	0.002479	-194.2	135.5
	398.43	0.01087	4.4	0.002510	-198.3	135.8
	393.48	0.006262	2.5	0.002541	-202.9	136.2
	388.54	0.003720	1.5	0.002574	-207.3	136.6
	383.62	0.002216	0.88	0.002607	-211.7	137.0
	378.68	0.001275	0.50	0.002641	-216.3	137.3
	373.72	0.0007515	0.29	0.002676	-220.8	137.7
	368.75	0.0004121	0.16	0.002712	-225.8	138.1
2	425.55	0.1417	59	0.002350	-176.7	133.8
	420.51	0.0895	37	0.002378	-180.5	134.2
	415.48	0.05611	23	0.002407	-184.5	134.6
	410.45	0.03518	14	0.002436	-188.4	134.9
	405.42	0.02140	8.7	0.002467	-192.6	135.3
	400.40	0.01297	5.3	0.002498	-196.8	135.7
	395.36	0.007835	3.2	0.002529	-201.0	136.1
	390.34	0.004578	1.8	0.002562	-205.6	136.4
	385.36	0.002748	1.1	0.002595	-209.9	136.8
	380.42	0.001545	0.61	0.002629	-214.7	137.2
3	428.08	0.1766	74	0.002336	-174.8	133.6
	423.05	0.1118	47	0.002364	-178.7	134.0
	418.03	0.07124	29	0.002392	-182.5	134.4
	413.00	0.04503	19	0.002421	-186.3	134.7
	407.99	0.02758	11	0.002451	-190.4	135.1
	402.98	0.01651	6.7	0.002482	-194.8	135.5
	397.96	0.01026	4.1	0.002513	-198.8	135.9

	392.95	0.006134	2.5	0.002545	-203.1	136.3
	387.99	0.003562	1.4	0.002577	-207.7	136.6
	383.08	0.002121	0.84	0.002610	-212.0	137.0

[PPy][NTf$_2$]

$$\ln(p^*_{\mathrm{sat}}/p^{\mathrm{o}}) = -\frac{73530}{RT_0} - \frac{127931}{R}\left(\frac{1}{T} - \frac{1}{T_0}\right) - \frac{66}{R}\left(\frac{T_0}{T} - 1 - \ln\left(\frac{T}{T_0}\right)\right),\ T_0 = 398.2\ \mathrm{K}$$

1	419.89	0.5316	163	0.002382	-168.2	126.5
	414.87	0.3452	105	0.002410	-171.9	126.8
	409.86	0.2220	67	0.002440	-175.6	127.2
	404.90	0.1426	43	0.002470	-179.3	127.5
	399.92	0.08893	27	0.002501	-183.3	127.8
	394.99	0.05599	17	0.002532	-187.2	128.1
	390.04	0.03413	10	0.002564	-191.4	128.5
	385.07	0.02065	6.1	0.002597	-195.6	128.8
	380.09	0.01213	3.5	0.002631	-200.1	129.1
	375.10	0.007137	2.1	0.002666	-204.5	129.5
2	422.39	0.6584	203	0.002367	-166.4	126.3
	417.38	0.4292	131	0.002396	-170.0	126.7
	412.40	0.2793	85	0.002425	-173.7	127.0
	407.44	0.1800	54	0.002454	-177.4	127.3
	402.49	0.1147	34	0.002485	-181.2	127.6
	397.54	0.07232	22	0.002515	-185.0	128.0
	392.59	0.04451	13	0.002547	-189.1	128.3
	387.61	0.02685	7.9	0.002580	-193.4	128.6
	382.62	0.01577	4.6	0.002614	-197.9	129.0
	377.65	0.009051	2.6	0.002648	-202.5	129.3

[BPy][NTf$_2$]

$\ln(p^*_{sat}/p^o) = -\frac{73466}{RT_0} - \frac{131039}{R}\left(\frac{1}{T} - \frac{1}{T_0}\right) - \frac{70}{R}\left(\frac{T_0}{T} - 1 - \ln\left(\frac{T}{T_0}\right)\right)$, T_0 = 399.5 K

1	422.34	0.6840	207	0.002368	-166.3	129.4
	417.37	0.4395	132	0.002396	-170.0	129.8
	412.37	0.2809	84	0.002425	-173.8	130.1
	407.40	0.1785	53	0.002455	-177.6	130.5
	402.45	0.1121	33	0.002485	-181.5	130.8
	397.50	0.07015	21	0.002516	-185.4	131.2
	392.53	0.04233	12	0.002548	-189.7	131.5
	387.56	0.02585	7	0.002580	-193.8	131.9
	382.58	0.01472	4	0.002614	-198.6	132.2
	377.61	0.008651	2	0.002648	-203.1	132.6
2	419.87	0.5557	168	0.002382	-168.0	129.6
	414.88	0.3549	106	0.002410	-171.8	130.0
	409.89	0.2254	67	0.002440	-175.6	130.3
	404.89	0.1410	42	0.002470	-179.6	130.7
	399.95	0.08834	26	0.002500	-183.5	131.0
	394.99	0.05354	16	0.002532	-187.7	131.4
	390.03	0.03283	10	0.002564	-191.8	131.7
	385.06	0.01946	5.6	0.002597	-196.2	132.1
	380.08	0.01132	3.2	0.002631	-200.8	132.4

[HEMIm][OTf]

$\ln(p^*_{sat}/p^o) = -\frac{72890}{RT_0} - \frac{129625}{R}\left(\frac{1}{T} - \frac{1}{T_0}\right) - \frac{71}{R}\left(\frac{T_0}{T} - 1 - \ln\left(\frac{T}{T_0}\right)\right)$, T_0 = 387.4 K

1	408.05	0.08510	124	0.002451	-170.5	128.2
	403.05	0.04998	73	0.002481	-175.0	128.5
	398.08	0.03027	44	0.002512	-179.2	128.9
	393.12	0.01851	27	0.002544	-183.3	129.2

	388.19	0.01095	16	0.002576	-187.8	129.6
	383.23	0.00673	10	0.002609	-191.9	129.9
	378.28	0.00386	5.4	0.002644	-196.5	130.3
	373.34	0.00213	3.0	0.002678	-201.5	130.6
	368.37	0.00124	1.7	0.002715	-206.1	131.0
	363.43	0.0007966	1.1	0.002752	-209.8	131.3
2	410.47	0.09862	144	0.002436	-169.2	128.0
	405.42	0.06012	88	0.002467	-173.4	128.3
	400.39	0.03619	52	0.002498	-177.7	128.7
	395.37	0.02236	32	0.002529	-181.7	129.1
	390.35	0.01368	20	0.002562	-185.9	129.4
	385.31	0.008126	12	0.002595	-190.3	129.8
	380.31	0.004905	6.9	0.002629	-194.5	130.1
	375.31	0.002843	4.0	0.002664	-199.1	130.5
	370.32	0.001718	2.4	0.002700	-203.3	130.8
	365.36	0.001013	1.4	0.002737	-207.8	131.2
3	413.00	0.1239	182	0.002421	-167.3	127.8
	407.95	0.07985	117	0.002451	-171.0	128.2
	402.92	0.04743	69	0.002482	-175.4	128.5
	397.90	0.02844	41	0.002513	-179.7	128.9
	392.87	0.01787	26	0.002545	-183.6	129.2
	387.84	0.01063	15	0.002578	-188.0	129.6
	382.80	0.006190	8.8	0.002612	-192.6	130.0
	377.81	0.003682	5.2	0.002647	-196.9	130.3
	372.81	0.002272	3.2	0.002682	-201.0	130.7
	367.85	0.001354	1.9	0.002718	-205.4	131.0

[HEMIm][NTf$_2$]

$$\ln(p^*_{\mathrm{sat}}/p^{\mathrm{o}}) = -\frac{74973}{RT_0} - \frac{122075}{R}\left(\frac{1}{T} - \frac{1}{T_0}\right) - \frac{65}{R}\left(\frac{T_0}{T} - 1 - \ln\left(\frac{T}{T_0}\right)\right),\ T_0 = 382.0\ \mathrm{K}$$

1	403.30	0.1415	42	0.002480	-179.5	120.7
	398.45	0.09086	27	0.002510	-183.3	121.0
	393.57	0.05912	17	0.002541	-186.9	121.3
	388.66	0.03772	10.9	0.002573	-190.7	121.6
	383.74	0.02320	6.7	0.002606	-194.8	122.0
	378.79	0.01437	4.1	0.002640	-198.8	122.3
	373.82	0.008561	2.4	0.002675	-203.2	122.6
	368.79	0.004842	1.4	0.002712	-208.0	122.9
	363.77	0.002859	0.80	0.002749	-212.4	123.3
	358.75	0.001577	0.44	0.002787	-217.4	123.6
2	406.02	0.1809	54	0.002463	-177.5	120.5
	401.29	0.1186	35	0.002492	-181.0	120.8
	396.46	0.07671	22	0.002522	-184.7	121.1
	391.54	0.04891	14	0.002554	-188.5	121.5
	386.56	0.02994	8.7	0.002587	-192.6	121.8
	381.56	0.01932	5.6	0.002621	-196.3	122.1
	376.54	0.01124	3.2	0.002656	-200.9	122.4
	371.49	0.006773	1.9	0.002692	-205.2	122.8
	366.41	0.003915	1.1	0.002729	-209.8	123.1
	361.34	0.002209	0.62	0.002768	-214.6	123.4

[HEMIm][OMs]

$$\ln(p^*_{\mathrm{sat}}/p^{\mathrm{o}}) = -\frac{81032}{RT_0} - \frac{136924}{R}\left(\frac{1}{T} - \frac{1}{T_0}\right) - \frac{71}{R}\left(\frac{T_0}{T} - 1 - \ln\left(\frac{T}{T_0}\right)\right),\ T_0 = 416.1\ \mathrm{K}$$

1	438.48	0.1616	68	0.002281	-175.5	135.4
	433.50	0.1017	43	0.002307	-179.4	135.7
	428.53	0.06544	27	0.002334	-183.1	136.1
	423.54	0.04201	17	0.002361	-186.8	136.4

	418.58	0.02627	11	0.002389	-190.8	136.7
	413.58	0.01670	6.8	0.002418	-194.6	137.1
	408.58	0.01024	4.2	0.002447	-198.7	137.4
	403.58	0.006282	2.5	0.002478	-202.8	137.8
	398.58	0.003742	1.5	0.002509	-207.2	138.1
	393.58	0.002257	0.90	0.002541	-211.4	138.5
2	440.75	0.1873	79	0.002269	-174.2	135.2
	435.71	0.1180	50	0.002295	-178.1	135.6
	430.66	0.07658	32	0.002322	-181.8	135.9
	425.63	0.04945	21	0.002349	-185.5	136.3
	420.46	0.03215	13	0.002378	-189.1	136.6
	415.43	0.02009	8.3	0.002407	-193.0	137.0
	410.44	0.01247	5.1	0.002436	-197.1	137.3
	405.46	0.007623	3.1	0.002466	-201.2	137.7
	400.54	0.004722	1.9	0.002497	-205.2	138.0
	395.65	0.002931	1.17	0.002528	-209.3	138.4
3	438.21	0.1553	66	0.002282	-175.8	135.4
	433.17	0.09861	41	0.002309	-179.6	135.7
	428.14	0.06373	27	0.002336	-183.3	136.1
	423.11	0.04119	17	0.002363	-187.0	136.4
	418.09	0.02538	10.5	0.002392	-191.1	136.8
	413.06	0.01600	6.6	0.002421	-195.0	137.1
	408.05	0.009883	4.0	0.002451	-199.0	137.5
	403.06	0.005984	2.4	0.002481	-203.2	137.8
	398.09	0.003484	1.4	0.002512	-207.8	138.2
	393.16	0.002107	0.84	0.002543	-212.0	138.5

[HEPy][NTf$_2$]

$\ln(p^*_{\mathrm{sat}}/p^{\circ}) = -\frac{79438}{RT_0} - \frac{134624}{R}\left(\frac{1}{T} - \frac{1}{T_0}\right) - \frac{81}{R}\left(\frac{T_0}{T} - 1 - \ln\left(\frac{T}{T_0}\right)\right)$, T_0 = 403.6 K

1	423.17	0.1065	33	0.002363	-181.6	133.0
	418.24	0.06977	21	0.002391	-185.2	133.4
	413.41	0.04385	13	0.002419	-189.1	133.8
	408.52	0.02833	8.6	0.002448	-192.7	134.2
	403.59	0.01771	5.3	0.002478	-196.7	134.6
	398.63	0.01045	3.1	0.002509	-201.1	135.0
	393.69	0.006467	1.9	0.002540	-205.2	135.4
	388.76	0.003860	1.1	0.002572	-209.5	135.8
	383.76	0.002246	0.66	0.002606	-214.1	136.2
	378.76	0.001265	0.37	0.002640	-218.9	136.6
2	426.41	0.1472	45	0.002345	-178.9	132.8
	420.81	0.08558	26	0.002376	-183.4	133.2
	415.82	0.05295	16	0.002405	-187.5	133.6
	410.85	0.03363	10	0.002434	-191.3	134.0
	405.87	0.02146	6.5	0.002464	-195.1	134.4
	400.90	0.01419	4.2	0.002494	-198.6	134.8
	395.94	0.008431	2.5	0.002526	-203.0	135.2
	390.99	0.004736	1.4	0.002558	-207.8	135.6
	385.99	0.003009	0.88	0.002591	-211.6	136.0
	381.04	0.001590	0.46	0.002624	-217.0	136.5
3	428.19	0.1713	53	0.002335	-177.6	132.6
	423.15	0.1101	34	0.002363	-181.3	133.0
	418.13	0.06893	21	0.002392	-185.3	133.4
	413.10	0.04401	13	0.002421	-189.0	133.9
	408.08	0.02744	8.3	0.002451	-193.0	134.3

	403.06	0.01623	4.9	0.002481	-197.4	134.7
	403.17	0.01624	4.9	0.002480	-197.4	134.7
	398.25	0.01011	3.0	0.002511	-201.4	135.1
	393.29	0.006135	1.8	0.002543	-205.6	135.5
	388.33	0.003591	1.1	0.002575	-210.1	135.9

[HPPy][NTf$_2$]

$$\ln(p^*_{\mathrm{sat}}/p^{\circ}) = -\frac{79817}{RT_0} - \frac{136787}{R}\left(\frac{1}{T} - \frac{1}{T_0}\right) - \frac{91}{R}\left(\frac{T_0}{T} - 1 - \ln\left(\frac{T}{T_0}\right)\right),\ T_0 = 412.5\ \mathrm{K}$$

1	433.17	0.1663	51	0.002309	-177.9	134.9
	428.21	0.11197	34	0.002335	-181.3	135.4
	423.35	0.07245	22	0.002362	-184.9	135.8
	418.48	0.04455	13	0.002390	-189.0	136.2
	413.62	0.02949	8.8	0.002418	-192.5	136.7
	408.73	0.01857	5.5	0.002447	-196.4	137.1
	403.84	0.01127	3.3	0.002476	-200.6	137.6
	398.94	0.006603	1.9	0.002507	-205.1	138.0
	394.01	0.003912	1.1	0.002538	-209.5	138.5
	389.06	0.002518	0.73	0.002570	-213.2	138.9
2	436.21	0.2259	69	0.002292	-175.4	134.6
	431.23	0.1449	44	0.002319	-179.1	135.1
	426.30	0.09634	29	0.002346	-182.5	135.5
	421.38	0.05913	18	0.002373	-186.6	136.0
	416.45	0.03817	11	0.002401	-190.3	136.4
	411.50	0.02322	6.9	0.002430	-194.5	136.9
	406.55	0.01417	4.2	0.002460	-198.7	137.3
	401.59	0.008873	2.6	0.002490	-202.6	137.8
	396.60	0.005386	1.6	0.002521	-206.8	138.2

	391.61	0.003379	0.98	0.002554	-210.7	138.7
3	436.07	0.2054	63	0.002293	-176.1	134.6
	431.12	0.1403	43	0.002320	-179.4	135.1
	426.21	0.09363	28	0.002346	-182.8	135.5
	421.28	0.06048	18	0.002374	-186.5	136.0
	416.37	0.03847	12	0.002402	-190.3	136.4
	411.45	0.02420	7.2	0.002430	-194.2	136.9
	406.51	0.01468	4.3	0.002460	-198.4	137.3
	401.56	0.008883	2.6	0.002490	-202.6	137.8
	396.60	0.005285	1.5	0.002521	-207.0	138.2
	391.61	0.003010	0.87	0.002554	-211.7	138.7

[a] the combined expanded uncertainties are $U_c(T) = 0.02$ K, $U_r(df \cdot dt^{-1}) = 0.01$ $U_r(p_{sat}) = 0.5$ for confidence level = 0.95, $k \approx 2$.

References:

1 S. P. Verevkin, D. H. Zaitsau, V. N. Emel`yanenko and A. Heintz, A new method for the determination of vaporization enthalpies of ionic liquids at low temperatures, *J. Phys. Chem. B*, 2011, **115**, 12889–12895.

2 G. Sauerbrey, Verwendung von Schwingquarzen zur Wägung dünner Schichten und zur Mikrowägung, *Z. Phys.*, 1959, **155**, 206–222.

3 D. H. Zaitsau, A. V Yermalayeu, V. N. Emel'yanenko, S. Butler, T. Schubert and S. P. Verevkin, Thermodynamics of imidazolium-based ionic liquids containing PF6 anions, *J. Phys. Chem. B*, 2016, **120**, 7949–7957.

4 E. C. W. Clarke and D. N. Glew, Evaluation of thermodynamic functions from equilibrium constants, *Trans. Faraday Soc.*, 1966, **62**, 539–547.

3. FT-IR Spectroscopy of the liquid phase

IR experiments for the condensed phase were performed on a TENSOR II FTIR spectrometer from BRUKER. The spectrometer uses a Globar® source, a KBr beam splitter and a DTGS room temperature detector. The sample cell was a demountable liquid cell with CaF_2-windows and a 12 µm Mylar®-spacer. For data collection analyses the OPUS 7.5 software was used. Every spectrum was accumulated for 128 scans with a resolution of 1 cm^{-1} and a 3 mm aperture. To avoid interference fringes, CCl_4 was used as background. The pure ILs were dried in vacuum to a water contend below 15 ppm. The ILs were prepared under SCHLENK-conditions in a 5 ml SCHLENK-tube in 2 g portions.

4 Molecular Dynamics Simulations

We did NpT molecular dynamics simulation using GROMACS 5.0.6 [1–5] at a temperature of $T = 300\,\mathrm{K}$ and a pressure of $p = 1\,\mathrm{bar}$. The ionic liquid was represented by a cubic simulation box containing 512 ion pairs. The box was first equilibrated for 2 ns at $T = 500\,\mathrm{K}$ employing the BERENDSEN thermostat as well as the BERENDSEN barostat [6] with coupling times of $\tau_\mathrm{T} = \tau_\mathrm{p} = 0.5\,\mathrm{ps}$. After that, another equlibration for 2 ns at the desired temperature of 300 K followed. Production runs of 100 ns length utilizing the NOSÉ-HOOVER thermostat [7, 8] with $\tau_\mathrm{T} = 1\,\mathrm{ps}$ and RAHMAN-PARRINELLO barostat [9, 10] with $\tau_\mathrm{p} = 2\,\mathrm{ps}$ were performed for each temperature.
The gas phase simulations were done on an ion pair of the corresponding ionic liquid. After equilibration over 2 ns at $T = 300\,\mathrm{K}$ production runs of 400 ns length were performed, employing the NOSÉ-HOOVER thermostat with $\tau_\mathrm{T} = 1\,\mathrm{ps}$.
All simulations were done with a 2.0 fs time step employing periodic boundary conditions and the LINCS algorithm [11] for fixed bond lengths. The smooth particle mesh EWALD summation [12] was applied in the liquid with a mesh spacing of 0.12 nm, a real space cutoff of 0.9 nm and 4th order interpolation. The relative accuracy of the EWALD sum was set to 10^{-5} corresponding to a convergence factor $\alpha = 3.38\,\mathrm{nm}^{-1}$.
The forcefield of the $[\mathrm{NTf_2}]^-$ anion is published in reference [13]. The forcefield of the $[\mathrm{PMIm}]^+$ cation is published in reference [14]. The forcefields of the other cations are described below.

4.1 $[\mathrm{HEPy}]^+$ Forcefield

The pyridinium forcefield was derived from the OPLS forcefield for pyridine from Jorgensen [15, 16]. The dihedral potentials of the hydroxyalkyl chain were fitted on ab initio calculations employing second order Møller-Plesset perturbation theory using the cc-pvtz basis set. The point charges were derived from the electostatic potential according to the CHelpG scheme [17]. All forcefield parameters for the $[\mathrm{HEPy}]^+$ cation can be found below.

SI Tab. S2: Lennard-Jones parameters σ and ϵ for all interaction sites of the $[HEPy]^+$ cation.

site	σ / Å	$\epsilon \cdot k_B^{-1}$ / K
N	3.25	85.55
C_a	3.55	35.23
H_a	2.42	15.10
C_c	3.50	33.20
H_c	2.50	15.10
H_m	2.50	15.10
O	3.12	85.60
H_o	0.00	0.00

SI Tab. S3: Bond length $r^0_{\kappa\lambda}$ and angle parameters $\phi^0_{\kappa\lambda\omega}$ und $k^a_{\kappa\lambda\omega}$ for the angle potential $V^a_{\kappa\lambda\omega} = \frac{1}{2}k^a_{\kappa\lambda\omega}(\phi_{\kappa\lambda\omega} - \phi^0_{\kappa\lambda\omega})^2$ in the force field of the $[HEPy]^+$ cation.

bond	$r^0_{\kappa\lambda}$ / Å	angle	$\phi^0_{\kappa\lambda\omega}$ / °	$k^a_{\kappa\lambda\omega}$ / kJ mol^{-1}rad^{-2}
C_a-N	1.339	C_a-C_a-C_a	120.0	527.20
C_a-H_a	1.080	C_a-C_a-N	124.0	585.80
C_a-C_a	1.400	C_a-N-C_a	117.0	585.80
N-C_c	1.339	C_a-C_a-H_a	120.0	292.90
C_c-C_c	1.529	N-C_a-H_a	116.0	292.90
C_c-H_c	1.090	C_a-N-C_c	121.5	585.80
C_c-O	1.410	N-C_c-C_c	112.7	487.43
O-H_o	0.945	H_c-C_c-N	110.7	313.26
C_c-H_m	1.090	H_c-C_c-H_c	107.8	275.70
		H_c-C_c-C_c	110.7	313.26
		H_m-C_c-C_c	110.7	313.26
		H_m-C_c-H_m	107.8	275.70
		C_c-C_c-C_c	112.7	487.43
		H_o-O-C_c	108.5	460.55
		C_c-C_c-O	109.5	418.68
		H_c-C_c-O	109.5	293.08

SI Tab. S4: Parameters m_n, k_m^{dp} and ψ_m^0 for the improper dihedral potential $V_{\kappa\lambda\omega\tau}^{\mathrm{dp}} = \sum_n k_m^{\mathrm{dp}}[1 + \cos(m_n\psi_m - \psi_m^0)]$ in the force field of the $[\mathrm{HEPy}]^+$ cation. The central atom is the first in the list.

	m_n	k_m^{dp} / kJ mol^{-1}	ψ_m^0 / °
N-C_a-C_a-C_c	2	4.6060	180.0
C_a-N-C_a-H_a	2	4.6060	180.0
C_a-C_a-C_a-H_a	2	4.6060	180.0

SI Tab. S5: Parameters m_n, k_m^{dp} and ψ_m^0 for the torsion potential $V_{\kappa\lambda\omega\tau}^{\mathrm{dp}} = \sum_n k_m^{\mathrm{dp}}[1+\cos(m_n\psi_m - \psi_m^0)]$ in the force field of the $[\mathrm{HEPy}]^+$ cation.

	$n(\kappa\lambda\omega\tau)$	m_n	k_m^{dp} / kJ mol^{-1}	ψ_m^0 / °
X-C_a-C_a-X	1	2	15.1780	180.0
X-C_a-N-X	1	2	15.1780	180.0
C_a-N-C_c-C_c	1	2	0.0802	0
	2	4	-0.4693	0
N-C_c-C_c-O	1	1	-0.7375	0.0
	2	2	1.8576	0.0
	3	3	7.2898	0.0
C_c-C_c-O-H_o	1	1	-5.8097	0.0
	2	2	1.8939	0.0
	3	3	2.5150	0.0

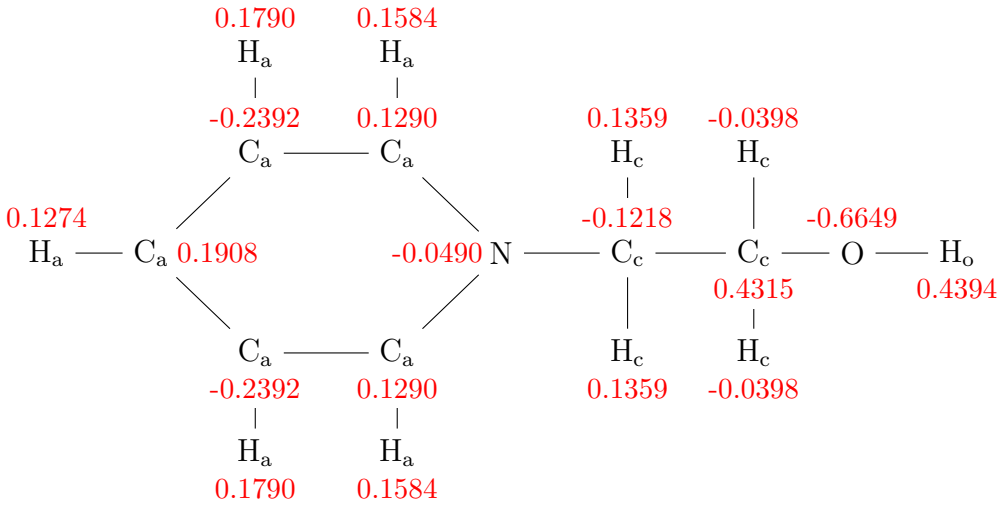

SI Fig. S1: Structure of the $[\mathrm{HEPy}]^+$ cation with atom types and corresponding point charges q/e in red.

4.2 $[PPy]^+$ Forcefield

The forcefield of the $[PPy]^+$ was derived similarly to the $[HEPy]^+$ forcefield. The parameters for the Lennard-Jones, bond, angle as well as the improper dihedral potential are the same and can be found in table 1 to 3 respectively. The dihedral potentials as well as the point charges can be found below.

SI Tab. S6: Parameters m_n, k_m^{dp} and ψ_m^0 for the torsion potential $V_{\kappa\lambda\omega\tau}^{\mathrm{dp}} = \sum_n k_m^{\mathrm{dp}}[1+\cos(m_n\psi_m - \psi_m^0)]$ in the force field of the $[PPy]^+$ cation.

	$n(\kappa\lambda\omega\tau)$	m_n	k_m^{dp} / kJ mol^{-1}	ψ_m^0 / °
X-C_a-C_a-X	1	2	15.1780	180.0
X-C_a-N-X	1	2	15.1780	180.0
C_a-N-C_c-C_c	1	2	-0.4178	0
	2	4	-0.4138	0
N-C_c-C_c-C_c	1	1	-1.4934	0.0
	3	3	6.8503	0.0
C_c-C_c-C_c-H_m	1	3	1.8318	0.0

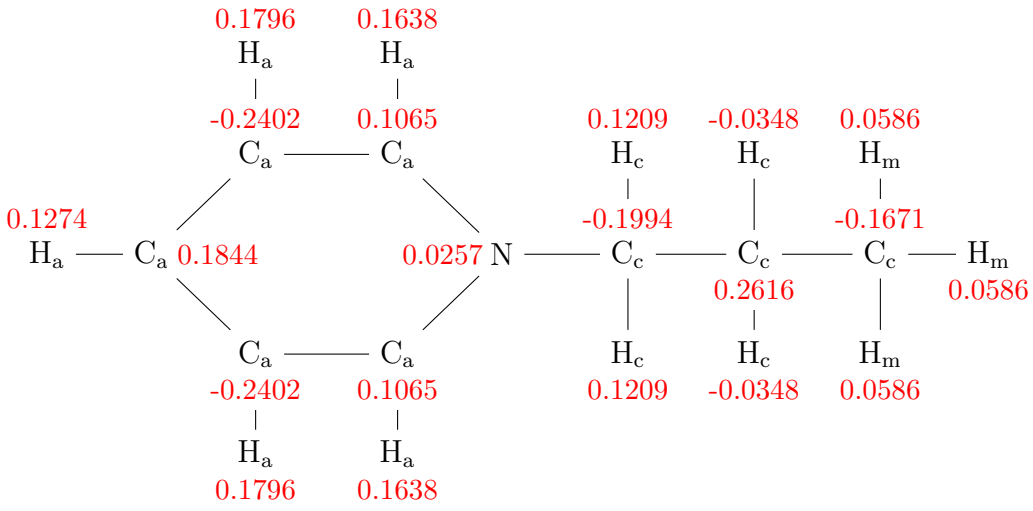

SI Fig. S2: Structure of the $[PPy]^+$ cation with atom types and corresponding point charges q/e in red.

4.3 $[HEMIm]^+$ Forcefield

The imidazolium forcefields are based on the forcefield from Kddermann et al. [14]. The dihedral potentials of the hydroxyalkyl chain were fitted on ab initio calculations employing second order Møller-Plesset perturbation theory using the cc-pvtz basis set. The original point charges on the ring atoms as well as the methyl group

were used. Only the point charges on the hydroxyalkl chain were calculated from the electostatic potential according to the Merz-Singh-Kollman scheme [18, 19] and scaled to give a resulting charge of the whole cation of +1 e. All forcefield parameters for the $[HEPy]^+$ cation can be found below.

SI Tab. S7: Lennard-Jones parameters σ and ϵ for all interaction sites of the $[HEMIm]^+$ cation.

site	σ / Å	$\epsilon \cdot k_B^{-1}$ / K
N	3.25	85.55
C_r	2.13	52.84
C_w	3.0175	24.66
H_a	1.452	22.65
H_b	2.057	10.60
C_1	3.50	33.20
C_c	3.50	33.20
H_1	2.50	15.10
H_c	2.50	15.10
O	3.12	85.60
H_o	0.00	0.00

SI Tab. S8: Bond length $r^0_{\kappa\lambda}$ and angle parameters $\phi^0_{\kappa\lambda\omega}$ und $k^{\mathrm{a}}_{\kappa\lambda\omega}$ for the angle potential $V^{\mathrm{a}}_{\kappa\lambda\omega} = \frac{1}{2}k^{\mathrm{a}}_{\kappa\lambda\omega}(\phi_{\kappa\lambda\omega} - \phi^0_{\kappa\lambda\omega})^2$ in the force field of the $[\mathrm{HEMIm}]^+$ cation.

bond	$r^0_{\kappa\lambda}$ / Å	angle	$\phi^0_{\kappa\lambda\omega}$ / °	$k^{\mathrm{a}}_{\kappa\lambda\omega}$ / kJ mol^{-1}rad^{-2}
C_c-C_c	1.529	C_c-C_c-C_c	112.7	487.43
C_c-H_c	1.090	H_c-C_c-H_c	107.8	275.70
C_1-H_1	1.090	H_c-C_c-C_c	110.7	313.26
C_c-O	1.410	H_1-C_1-C_1	107.8	275.70
O-H_o	0.945	H_1-C_1-N	110.7	313.26
C_w-C_w	1.341	H_C-C_C-N	110.7	313.26
N-C_1	1.466	C_1-N-C_r	126.4	292.60
N-C_c	1.466	C_1-N-C_w	125.6	292.60
C_w-N	1.378	C_c-N-C_r	126.4	292.60
C_r-N	1.315	C_c-N-C_w	125.6	292.60
C_r-H_a	1.080	H_a-C_r-N	125.1	146.30
C_w-H_b	1.080	H_b-C_w-N	122.0	146.30
		H_b-C_w-C_w	130.9	146.30
		H_o-O-C_c	108.5	460.55
		C_c-C_c-O	109.5	418.68
		H_c-C_c-O	109.5	293.08

SI Tab. S9: Parameters m_n, k^{dp}_m and ψ^0_m for the improper dihedral potential $V^{\mathrm{dp}}_{\kappa\lambda\omega\tau} = \sum_n k^{\mathrm{dp}}_m[1 + \cos(m_n\psi_m - \psi^0_m)]$ in the force field of the $[\mathrm{HEMIm}]^+$ cation. The central atom is the first in the list.

	m_n	k^{dp}_m / kJ mol^{-1}	ψ^0_m / °
N-C_w-C_r-C_1	2	9.20	180.0
C_r-N-N-H_a	2	9.20	180.0
C_w-C_w-N-H_b	2	8.37	180.0

SI Tab. S10: Parameters m_n, k_m^{dp} and ψ_m^0 for the torsion potential $V_{\kappa\lambda\omega\tau}^{\mathrm{dp}} = \sum_n k_m^{\mathrm{dp}}[1+\cos(m_n\psi_m - \psi_m^0)]$ in the force field of the $[\mathrm{HEMIm}]^+$ cation.

	$n(\kappa\lambda\omega\tau)$	m_n	k_m^{dp} / kJ mol^{-1}	ψ_m^0 / °
X-N-C_r-X	1	2	19.46	180.0
X-C_w-C_w-X	1	2	44.98	180.0
X-N-C_w-X	1	2	12.55	180.0
C_w-N-C_1-H_1	1	3	0.55	0
C_r-N-C_c-C_c	1	2	1.8560	0
	2	3	-0.6785	0.0
	3	4	-0.5112	0.0
N-C_c-C_c-O	1	1	-1.9592	0.0
	2	2	1.0784	0.0
	3	3	7.08193	0.0
	4	4	0.5216	0.0
C_c-C_c-O-H_o	1	1	-3.3455	0.0
	2	2	1.9342	0.0
	3	3	2.5818	0.0

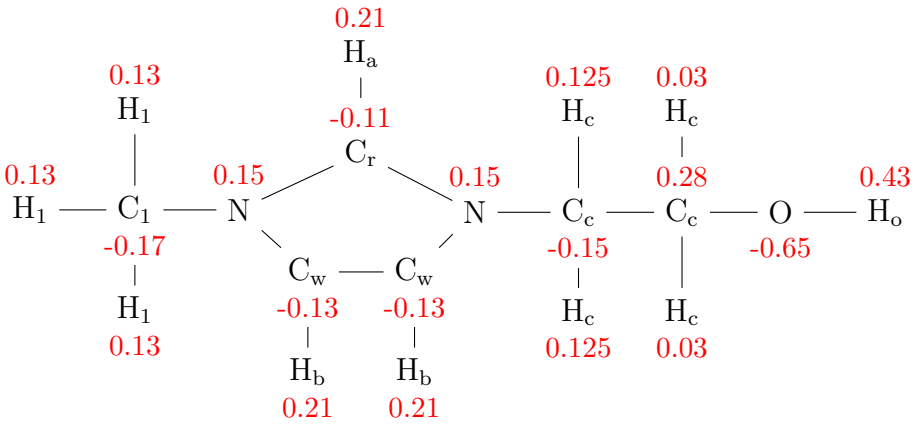

SI Fig. S3: Structure of the $[\mathrm{HEMIm}]^+$ cation with atom types and corresponding point charges q/e in red.

References

[1] E. Lindahl, B. Hess, D. van der Spoel, "Gromacs 3.0: A package for molecular simulation and trajectory analysis", *J. Mol. Mod.* **2001**, *7*, 306–317.

[2] H. J. C. Berendsen, D. van der Spoel, R. van Drunen, "Gromacs: A Message-Passing Parallel Molecular Dynamics Implementation", *Comp. Phys. Comm.* **1995**, *91*, 43–46.

[3] B. Hess, C. Kutzer, D. van der Spoel, E. Lindahl, "Gromacs 4: Algorithms for highly efficient, load-balanced, and scalable molecular simulation", *J. Chem. Theory Comput.* **2008**, *4*, 435–447.

[4] S. Pronk, S. Pall, R. Schulz, P. Larsson, P. Bjelkmar, R. Apostolov, M. R. Shirts, J. C. Smith, P. M. Kasson, D. van der Spoel, B. Hess, E. Lindahl, "Gromacs 4.5: A high-throughput and highly parallel open source molecular simulation toolkit", *Bioinformatics* **2013**, *29*, 845–54.

[5] M. Abraham, B. Hess, D. van der Spoel, E. Lindahl, E. Apol, R. Apostolov, H. J. C. Berendsen, A. van Buuren, P. Bjelkmar, R. van Drunen, A. Feenstra, S. Fritsch, G. Groenhof, C. Jungshans, J. Hub, P. Kasson, C. Kutzner, B. Lambeth, P. Larsson, J. A. Lemkul, E. Marklund, P. Meulenhoff, T. Murtola, S. Pall, S. Pronk, R. Schulz, M. Shirts, A. Sijbers, P. Tieleman, C. Wennberg, M. Wolf, Gromacs 5.0.6, **2015**.

[6] H. J. C. Berendsen, J. P. M. Postma, W. F. van Gunsteren, A. DiNola, J. R. Haak, "Molecular dynamics with coupling to an external bath", *J. Chem. Phys.* **1984**, *81*, 3684–3690.

[7] S. Nosé, "A molecular dynamics method for simulating in the canonical ensemble", *Mol. Phys.* **1984**, *52*, 255–268.

[8] W. G. Hoover, "Canonical Dynamics: Equilibrium Phase space distributions", *Phys. Rev. A* **1985**, *31*, 1695–1697.

[9] M. Parrinello, A. Rahman, "Polymorphic transitions in single crystals: A new molecular dynamics method", *J. Appl. Phys.* **1981**, *52*, 7182–7180.

[10] S. Nosé, M. L. Klein, "Constant pressure molecular dynamics for molecular systems", *Mol. Phys.* **1983**, *50*, 1055–1076.

[11] B. Hess, H. Bekker, H. J. C. Berendsen, J. G. E. M. Fraaije, "LINCS: A linear constraint solver for molecular simulations", *J. Comp. Chem.* **1997**, *18*, 1463–1472.

[12] U. Essmann, L. Perera, M. L. Berkowitz, T. A. Darden, H. Lee, L. G. Pedersen, "A smooth particle mesh Ewald method", *J. Chem. Phys.* **1995**, *103*, 8577–8593.

[13] J. Neumann, B. Golub, L.-M. Odebrecht, R. Ludwig, D. Paschek, "Revisiting imidazolium based ionic liquids: Effect of the conformation bias of the [ntf2] anion studied by molecular dynamics simulations", *The Journal of Chemical Physics* **2018**, *148*, 193828.

[14] T. Köddermann, D. Paschek, R. Ludwig, "Molecular dynamic simulations of ionic liquids: A reliable description of structure, thermodynamics and dynamics", *ChemPhysChem* **2007**, *8*, 2464–2470.

[15] W. L. Jorgensen, D. S. Maxwell, J. Tirado-Rives, "Development and testing of the OPLS all-atom force field on conformational energetics and properties of organic liquids", *Journal of the American Chemical Society* **1996**, *118*, 11225–11236.

[16] W. L. Jorgensen, N. A. McDonald, "Development of an all-atom force field for heterocycles. Properties of liquid pyridine and diazenes", *Journal of Molecular Structure: THEOCHEM* **1998**, *424*, 145–155.

[17] C. M. Breneman, K. B. Wiberg, "Determining atom-centered monopoles from molecular electrostatic potentials. The need for high sampling density in formamide conformational analysis", *Journal of Computational Chemistry* **1990**, *11*, 361–373.

[18] U. C. Singh, P. A. Kollman, "An approach to computing electrostatic charges for molecules", *Journal of Computational Chemistry* **1984**, *5*, 129–145.

[19] B. H. Besler, K. M. Merz Jr, P. A. Kollman, "Atomic charges derived from semiempirical methods", *Journal of Computational Chemistry* **1990**, *11*, 431–439.